Polytechnic Journal

Polytechnic Journal

Volume 13 | Issue 1 Article 10

Nonlinear analysis of pile raft foundations under eccentric loads

Khalid Qasim Hussein

Dept.of Civil Engineering,College of Engineering, Duhok University, Duhok, Kurdistan Region, Iraq, khalidqasimeng1990@gmail.com

Dr. Rafi' M. Sulaiman Al-Ne'aimi

Department of Civil Engineering, College of Engineering, Duhok University, Duhok, Kurdistan Region, Iraq

How to Cite This Article

Hussein, Khalid Qasim and Al-Ne'aimi, Dr. Rafi' M. Sulaiman (2023) "Nonlinear analysis of pile raft foundations under eccentric loads," *Polytechnic Journal*: Vol. 13: Iss. 1, Article 10.
DOI: https://doi.org/10.59341/2707-7799.1734

Polytechnic Journal. 2023. 13(1)
ISSN: 2313-5727
http://journals.epu.edu.iq/index.php/polytechnic

RESEARCH ARTICLE

Nonlinear analysis of pile raft foundations under eccentric loads

Khalid Qasim Hussein[1*], Dr. Rafi' M. Sulaiman Al-Ne'aimi[2]

[1] *Department of Civil Engineering, College of Engineering, Duhok University, Duhok, Kurdistan Region, Iraq*

[2] *Department of Civil Engineering, College of Engineering, Duhok University, Duhok, Kurdistan Region, Iraq*

***Corresponding author:**
Khalid Qasim Hussein,
Dept. of Civil Engineering,
College of Engineering,
Duhok University, Duhok,
Kurdistan Region, Iraq

E-mail:
khalidqasim.eng1990@gmail.com

Received: 27 Oct. 2022
Accepted: 9 May2023
Published:20 September 2023

DOI: https://doi.org/10.59341/2707-7799.1734

ABSTRACT

This paper discusses a series of 3D nonlinear analyses of the pile group foundation of a 34-floor multi-story building subjected to vertical load and large moments using PLAXIS 3D v20 software. The soil profile consists of seven strata of various properties, with groundwater encountered at 19.6 m below the ground surface. The soil is modeled as hardening soil material in drained conditions. The piles in the pile group foundation are modeled as embedded pile elements. Several parameters were investigated through a rigorous parametric study, such as the pile spacing-diameter ratio *(s/d_{pile})*, the number of piles, and the pile slenderness ratio *(l/d_{pile})* in a square pile configuration with all piles of equal length, on the behavior of un-piled and pile raft foundations of rectangular shape in the plan under eccentric load. The analysis's results were thoroughly examined and discussed, and several conclusions were presented.

Key Words: Finite element, Pile rafts, Constitutive model, Numerical analysis, Large moments.

1-INTRODUCTION

In designing a foundation, raft foundations are usually the first option to support superstructure loads. If these

foundations cannot satisfy the design requirements of settlement and bearing capacity, pile raft foundations are used instead to transmit the structural loads to a deeper
stratum through a pile cap that is connected to the piles at

their heads. In general, piles are used in groups that are arranged in different layout patterns such as square, triangular, etc. and are installed fairly close together with a minimum distance between centers of $s=3d_{pile}$ for heavy structures or high-rise buildings. For distributing the load more uniformly among piles in a group, large spacing between piles is often impractical. In design a pile group foundation with the pile cap is fully rigid and is not in contact with underlying soil, in addition to the piles modeled as springs of the same flexural stiffness, EI, and fixed bases as shown in Fig. 1, the applied loads and
moments are transmitted only to the piles, and the load carried by each pile under eccentric load can be

$$Pn = \frac{\sum P_n}{n} \pm \frac{\sum Mu_{yy}}{Iy} \overline{xn} \pm \frac{\sum Mu_{xx}}{Ix} \overline{yn} \quad \ldots\ldots\ldots\ldots\ldots\ldots\ldots\ldots (1)$$

where, Pn = pile load, $\sum P_n$ = total ultimate vertical load, $\sum Mu_{yy}$ $\sum Mu_{xx}$= These are the ultimate moments about the x and y axes, xn, yn = The distance between any pile and the y- and x-axes, and Iy =$\sum_i x^2$, Ix =$\sum_i y^2$= Group moment of inertia.

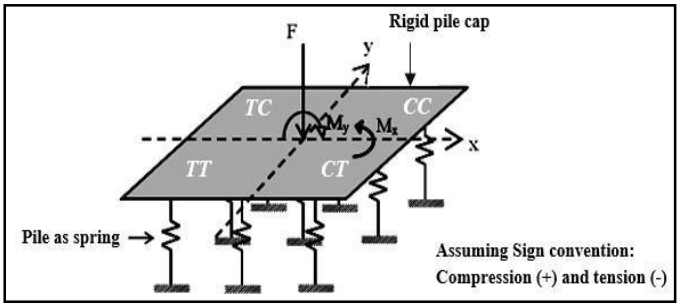

Foundations based on piled rafts have complex behavior, which depends on how the raft, piles, and subsoil interact. This system requires a raft foundation that is safe from soil-bearing failure, and piles designed to reduce settlements to an acceptable level.

There have been several studies using 2D and 3D (FEM) numerical tools to examine the effects of raft thickness, pile configuration, pile number, and pile length on piled raft foundations. Using a typical geotechnical engineering problem under vertical loads, Prakoso and Kulhawy (2001) examined the impact of raft and pile group geometries on total and differential settlements, as well as raft bending moments. It was found that Comodromos et al. (2003) conducted a back analysis of pile load testing to determine the load-settlement relationship between different layouts of a pile group. As the pile spacing decreased, the pile interaction increased, which resulted in less stiffness for each pile. In addition, Tomlinson and Woodward (2007) assert that pile raft depths vary based on soil type and are typically about 2/3L for floating piles and L for tip piles. Assuming that the load is transferred to the subsoil via the pile's shaft by skin friction in the proportion of 1H:4V and the vertical stress is spread in the proportion of 2V:1H on a thick hard layer or rock, settling analysis is not needed for piles resting on thick hard rock. Approximately 50–80% of the overall weight of pile rafts is carried by piles, according to Davids et al. (2008).

Based on 2D analyses, Rabiei (2010) concluded that a limited number of piles beneath the raft can be used to limit the raft's bearing capacity and settlement. As the raft thickness increases and the pile's length or number decreases, the maximum bending moment of the raft increases, while total and differential settlements decrease. The piled raft is a three-dimensional problem, according to Ryltenius (2011), and the 2D analysis overestimates the raft's settlement and moment by 30% and its pile load by 10%. Furthermore, the 2D model resembles the 3D model more closely as the pile spacing decreases. Gebregziabher and Katzenbach (2012) found that pile spacing, length, and layout are important factors that influence piled raft foundation settlement and load sharing. Load sharing between the piles and raft is further enhanced when the piles are widely separated.

Based on centrifuge model testing, Choudhury et al. (2008) found that the maximum negative bending moment at pile heads occurred when four piles were attached at their heads to the pile caps of variable stiffness. Furthermore, a pile group with a flexible pile cap displayed higher pile head deflection than a pile group with a rigid pile cap. Fioravante and Giretti (2010) tested a piled-raft foundation in sand using centrifugal forces. There is a direct connection between the stiffness of the pile-soil system and the amount of load shared between the piles and the raft in the rigid raft, whereas those in the flexible raft can minimize both overall and differential settlements.

During pile raft foundation construction, the pile cap or raft is placed directly on the ground and attached directly to the pile heads. Through the raft and piles, part of the superstructure load is transmitted directly to the subsurface. Viggiani et al. (2012) examined the load-sharing among piles of high-rise buildings in soft clay and concluded that the piled raft system is also adequate in terms of bearing capacity and serviceability. According to their findings, the corner and side piles of a group absorb more loads as their spacing decreases, despite the distribution of values. The raft soil contact absorbs about 70% of the applied load at s/d_{pile} =12, whereas a reverse trend is observed in piled rafts. Based on the soil conditions under the earth, Abdel-Fattah and Hemada (2014) find that 30–60% of the total superstructure load is transferred to the soil by the raft contact pressure. In addition to decreasing the length of the piles and increasing the spacing of the piles, this percentage increases. As Tang et al. (2014) noted, when the pile spacing diameter ratio (s/d_{pile}) > 5, each raft and pile can behave independently, reaching their full bearing capacity. The three foundation options identified by Elwakil and Azzam (2016) were raft foundations, where loads are transferred to the subsoil via the raft; pile foundations, where loads are transferred to the ground through piles; and pile raft foundations, which transfer loads to the ground through piles and rafts. Sales et al. (2017) assessed pile group behavior under vertical loads, considering settlement, bearing capacity, and pile load distribution, using monitoring data of full-scale structures and experimental models. In conclusion, the classical method used in practice for foundation design cannot be applied to a proper design and will need to be revised.

The authors of Sivrikaya and Gurkan (2019) investigated piled-raft foundations with different pile spacings in clay soil using the PLAXIS 2D and 3D packages. Comparing the 2D and 3D modeling analyses reveals the dimension effect. They report a significant decrease in displacements, shears, and volumes when the pile spacing s/dpile increased, but not for $s/d_{pile} \geq 6$. In a study by Al-Ne'aimi and Hussain (2021), using the 3D foundation code, they examined the behavior of unpiled and piled square rafts subjected to uniform vertical loads varying the thickness of the rafts and the number, spacing, and diameter of the piles. Assuming drained soil conditions, we use the MC model to model the soil as an elastoplastic, while we model the piles as embedded volume elements. Increasing pile diameter resulted in the piles absorbing more loads than the raft, resulting in less settlement and bending moment for the raft. Moreover, for

all t rafts tested, the central piles absorb the most load of all nine pile group rafts of d_{pile} = 0.5 m or 0.6 m, and the edge and corner piles absorb the least load of all nine pile group rafts. The opposite trend is found in group rafts of 25 piles.

In this study, the behavior of unpiled and piled-raft foundations (with square pattern pile groups of equal length) of a multistory building of rectangular shape in plan and subjected to a combined vertical load and large moments was investigated through an extensive parametric study using the PLAXIS 3D v20 code.

2- Method of Analysis

2-1 3D Finite element software

A numerical analysis of this study was carried out using PLAXIS 3D v20 software. A professional finite element computer program was developed for studying and solving deformation problems in geotechnical engineering, including static and dynamic 3D nonlinear finite elements. In addition, the software features can deal with varying aspects of complex geotechnical structures, including elastoplastic deformation analysis of advanced soil models and soil-structure interaction issues where fully structural models are available, including plate elements, beam elements, and special elements called volume piles and embedded piles for modeling piles in a pile group foundation.

2-2 Constitutive modeling

Hardening-soil model (HSM) is the constitutive model used to simulate soil layers. An Obrzud (2010) model which is linear-elastic and perfectly plastic reproduces soil deformations more accurately. It includes three different input stiffness parameters, which results in a non-linear relationship between stress and strain (see Fig. 2). It can simulate the shear plastic strains observed in granular soils and over-consolidated cohesive soils, and the compressive plastic strains observed in soft soils, since it incorporates two hardening mechanisms.

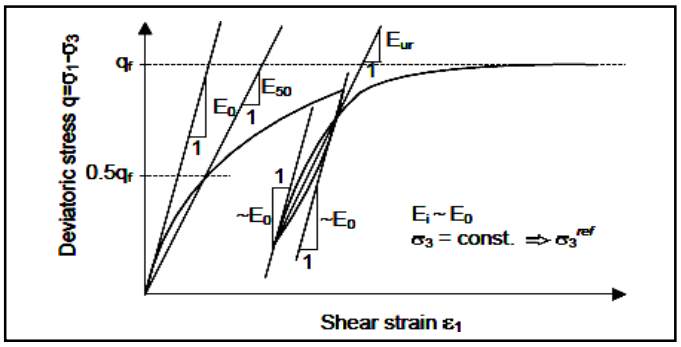

Fig. 2 Hyperbolic stress-strain relationship with definitions of different moduli of hardening soil small strain model (Plaxis 3D manual, 2013).

2-3 Model geometry boundaries and mesh generation

Yongdingmen Station's soil profile was used in this study as reported by Li et al. (2020), At the model's center is a single borehole that specifies a 44 m depth of soil composed of seven different types. A groundwater level of 19.6 m is located below the surface of the ground. As can be seen in the figure below Fig. 3, the soil profile and its properties can be found.

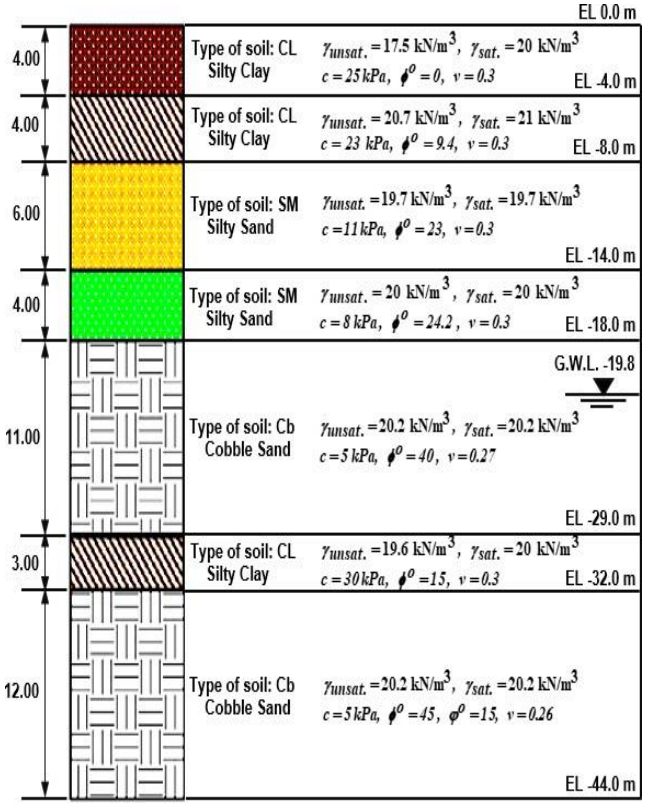

Fig. 3 Soil layers' profile used in this analysis (after Li, et al. (2020).

Three material components are included in the numerical model: soil elements, embedding pile elements, and pile cap plate elements. At the bottom boundary of the model, all directions x, y, and z are fixed, but not in the side boundary. A fully automatic mesh generation is performed after the soil and structural models, loads, and boundaries have been defined. Based on the geometry of the model, PLAXIS generates a 2D mesh of 6-node triangular elements. A 3D mesh showing soil stratigraphy and structure levels was automatically generated from the 2D mesh. To get accurate results, the global coarseness must be adjusted to fine mesh refinement with a global scale factor of 0.5. In Fig. 4, you can see many views of the geometry model and meshing for the 6x10 piled-raft foundation case with a 20-m pile length and s/d_{pile} = 3.

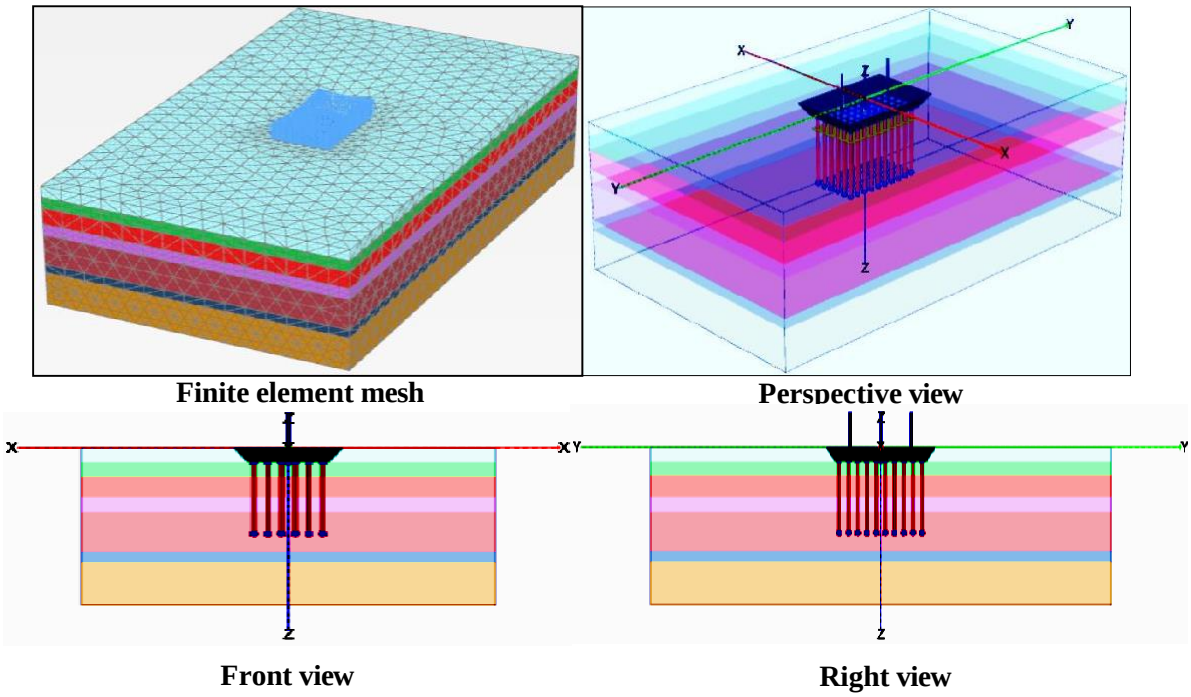

Fig. 4 Many views of the geometry model of the 6x10 pile group foundation (L20 m and S/d = 3).

The soils are discretized by the 10-noded tetrahedral element, nodes have three degrees of freedom for translation. There are six nodes in the plate modeling the pile cap, which has three translational degrees of freedom and three rotational degrees of freedom. Plate elements are formulated using Mindlin's plate theory, Bathe (1996). An embedded pile line element with three translational and three rotational degrees of freedom is used to model piles Engin et al. (2008) and Engin et al. (2007). A linear-elastic, non-porous material is modeled for each pile cap and pile. As shown in Fig. 5, the soil and structural elements are schematically represented. According to Table 1, soil parameters are shown for each soil layer, and structural properties are presented for the raft and piles are presented in Table 2.

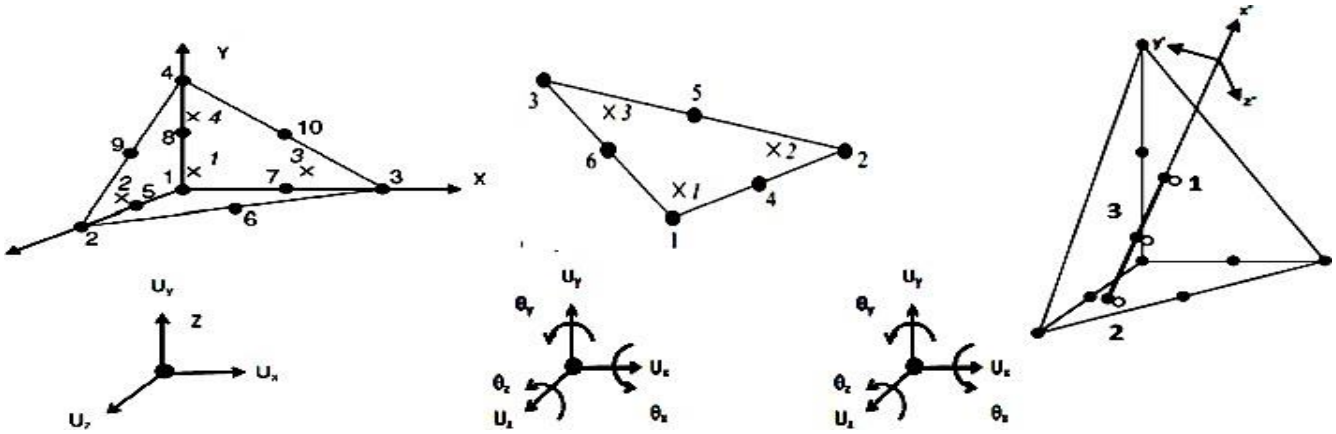

Fig. 5 Types of element and their degrees of freedom in PLAXIS 3D (PLAXIS 3D Connect v20 - scientific manual).

Table 1: Parameters of the soil layers for hardening soil model (HSM) analysis (after Li et al. (2020)).

Parameter	Soil type layers						
	SM	CL	SM	SM	Cb	CL	Cb
Thickness (m)	4	4	6	4	11	3	12
Material model	HS	HS	HS	HS	HS	HS	HS
Analysis type	Drained	Drained	Drained	Drained	Drained	Drained	Drained
Unit weight, γ_{unsat}(kN/m^3)	18.35	20.7	19.7	20	20.2	19.6	20.2
Saturated unit weight, γ_{sat} (kN/m^3)	20	21	20.2	21	21	20.2	21
Initial void ratio, e_0	0.6	0.6	0.6	0.6	0.6	0.6	0.6
Secant stiffness from a drained triaxial test, E_{50}^{ref} (MPa)	18.35	22.44	23.01	31.22	132	32.08	198
Tangent stiffness for oedometer primary loading, E_{oed}^{ref} (MPa)	18.35	22.44	23.01	31.22	132	32.08	198
Unloading/reloading stiffness, E_{ur}^{ref} (MPa)	55.04	67.32	69.30	63.65	396	96.23	594
Rate of stress dependency, m	0.5	1	0.5	1	1	0.5	1
Cohesion, c' (kPa)	0	23	11	8	5	30	5
Internal friction angle, ϕ^0	21.4	9.4	23	24.2	40	15	45
Dilatancy angle, φ^0	0	0	0	0	10	0	15
Unloading/reloading Poisson's ratio, ν_{ur}	0.3	0.3	0.3	0.3	0.27	0.3	0.26
Coefficient of earth pressure at rest (NC state), $K_0^{nc} = 1 - \sin\ \phi^o$	0.64	0.84	0.61	0.59	0.35	0.74	0.29
Failure ratio, R_f	0.9	0.9	0.9	0.9	0.9	0.9	0.9
Interface reduction factor, R_{inter}	0.8	0.8	0.8	0.8	1.0	0.7	1.0
Over-consolidation ratio, OCR	1.0	1.0	1.0	1.0	1.0	1.0	1.0

Table 2: Material properties of the pile cap (raft) and the embedded pile (after Al-Ne'aimi and Hussain (2021)).

Parameter	Pile cap	Embedded Pile	
Material model	Linear-elastic	Linear-elastic	
Material type	Non-porous	Non-porous	
Element type	Plate	Beam	
Young's modulus, E (MN/m^2)	3.0 x 10^4	2.92 x 10^4	
Poisson's ratio, ν	0.2	0.3	
Unit weight, γ (kN/m3)	25	25	
Thickness, t_{raft} (m)	2	-------	
Diameter, d_{pile} (m)	-------	1.0	
Length, L_{pile} (m)	-------	12, 16, 20	
Interface reduction factor, R_{inter}	1.0	1.0	
Axial skin resistance	-------	Multi-linear*	
Multi-linear axial resistance		L	Tmax (kN/m)
		0	0
		4.0	96.5
		10.0	225
		14	285
		20	436
End-bearing resistance, F_{max} (kN)		4107,15930,15930	

*All skin friction and end-bearing values are obtained from PROKON v3.0

As shown in Table 2, the input data for embedded pile elements consist of:

- The pile's beam properties are the stiffness and weight of the material, as well as the shape and dimensions of the cross-section.
- There are three properties of coupling springs: the interface normal stress remains elastic (unlimited by any failure law); the interface shear stress is determined by the ultimate traction value Tmax along the pile shaft, and the pile end-bearing resistance is determined by the value Fmax of a linear elastic-perfectly plastic spring in the pile axial direction.

2-4 Validation of the finite element model

The results obtained by Al-Ne'aimi and Hussain (2021) for 10-m square un-piled and piled raft foundations loaded with a vertical uniform load of 430 kN/m2 using Plaxis 3D Foundation have been taken for validation of numerical modeling. There are five layers of soil with various properties within the soil profile, with groundwater at -3.5 m below the surface. Using the Mohr-Coulomb model in drained conditions, soil is treated as elastoplastic material, while piles are treated as embedded volume elements. For more information on the soil profile, the raft, and piles, refer to Al-Ne'aimi and Hussain (2021). During the prototype testing, nine piles of 0.5 m diameter and 18 m length made up the piled rafts with thicknesses of 1.0, 1.5, and 2.0 m. The piles were arranged in a 3×3 square pattern with uniform spacing equal to four times the pile diameter, that is, $s/d_{pile} = 4$.

According to Fig. 6, un-piled raft and 3x3 piled raft foundation load-settlement curves are shown in a, b, c, and d. From both a trend and magnitude standpoint, the load-settlement curves obtained from the present model appear to be similar to those obtained through the Plaxis 3D

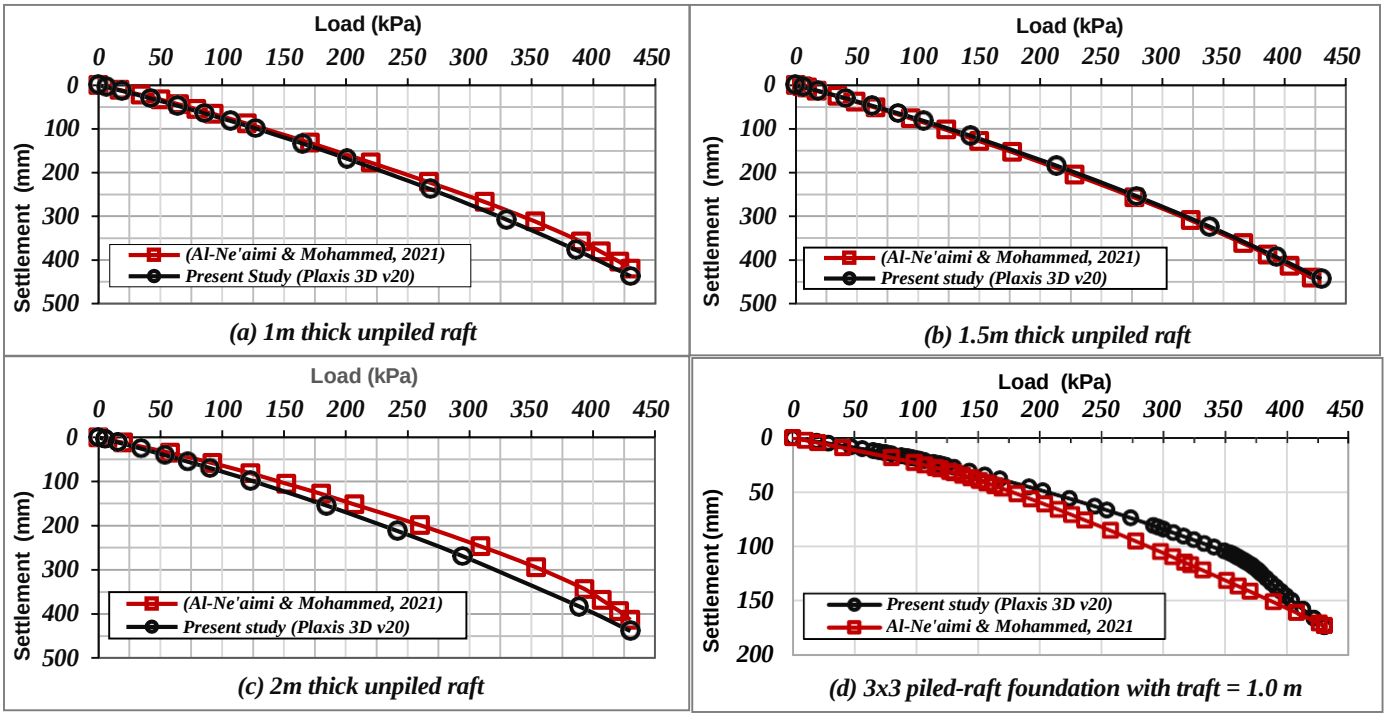

Fig. 6 Validation of the Plaxis 3D v20 with the 3D Foundation v1.6 result for un-piled raft and 3×3 pile-raft foundation

3- Parametric study

The effect of pile spacing-diameter ratio was investigated in this study (*s/dpile*), The number of piles, the ratio of slenderness of piles (*l/dpile*), and moment load in a square pattern layout pile group with all piles of equal length, on the pile load distribution and the behavior of a rectangular raft-supported pile of a 34-floor multistory building under vertical load and large moments were investigated. The results are then to be compared with that of the unpiled raft case. The pile cap area is 18m x 30m and *traft* = 2.0 m. A maximum load of 15 kN/m2 (dead and live) has been assumed. As a result, for the chosen case of a 34-story building, the total load applied to the raft or pile cap foundation as a distributed load for the structure would be 510 kN/m2. The moments applied at the center of the foundation are M_x=−50000 kN-m and M_y=30000 kN-m. Consequently, for the rectangular pile cap area (18x30 = 540 m2). As a result, the structure's maximum design load is 275.4 MN. Details of the testing program schedule with varying studied parameters are shown in Table 3. The studied piled rafts for raft thicknesses of 2.0 m and 24, 40, and 60 piles for one set of study cases are shown in Fig.7.

3-1 Sequence of analysis

The calculation process of the model consists of four phases defined according to the sequence of structure construction and loading in the staged construction mode as follows:

- The first stage of analysis corresponds to the initial stress state calculated by using the K_O procedure, while the pore water pressure is calculated following a hydrostatic condition. At this stage, only soil elements are activated in the model.

- Excavation is the second stage of the calculation. The surfaces of the excavation have been aligned vertically (3H/4V) to prevent "soil body collapse" at the edges.

- Third is the construction of a raft foundation based on piled rafts. All structural elements, including plate elements, embedded piles, and boundary conditions, are activated in the staged construction mode with the plastic calculation type and default iterative procedure setting. Long-term settlements are considered using the drained type analysis.

- Fourth, the pile cap axes are activated by the vertical loads and moments applied along their axes.

Once all stages are set up and defined, a nonlinear elastic-plastic deformation analysis is performed from the second stage to the final one. An iterative procedure with automatic load-stepping control is used for each stage. The program will automatically use the most appropriate numerical procedure and proper selection of load steps to determine a nonlinear finite element solution. On multi- core processors, all analyses are performed using the default numerical approach, Picos, which solves sparse linear equations in parallel. Using the implicit stress integration algorithm, stress increments are obtained at each integration point for known strain increments. In the PLAXIS 3D Connect v20 reference manual, you can find more information about Picos and stress integration.

Table 3: Details of the testing program schedule.

Series no.	Load condition	Case study	t_{raft} (m)	$S/_{pile}$	L/d_{pile}	Number of piles	Number of tests
1	Static load V = 510 kPa	Unpiled raft 18m ×30m	2.0	------	------	------	1
2	Mx =−50000 kN-m My = +30000 kN-m Mz = 0 kN-m	Piled raft 18m ×30m	2.0	5,4,3	12,16,20 equal lengths	24, 40, 60 22, 36, 56	18

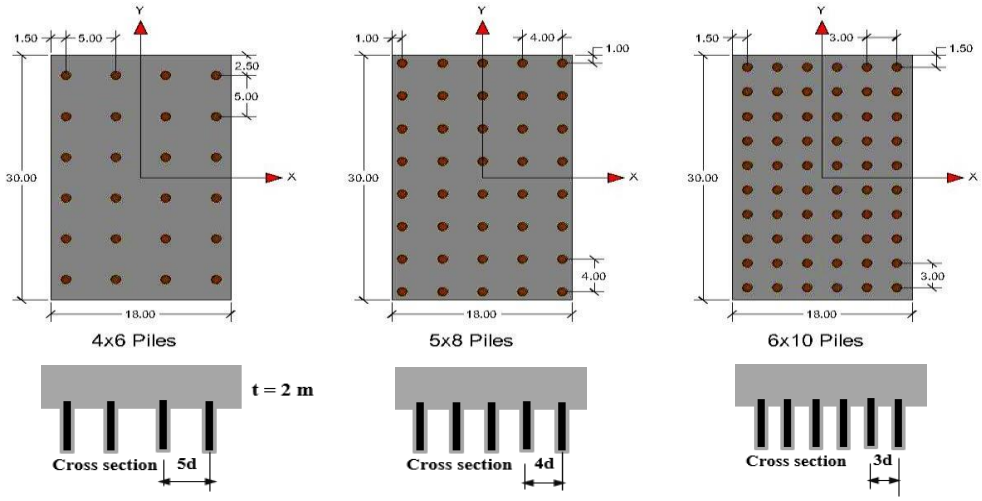

Fig. 7 Studied rafts-supported piles for 24, 40, 60 piles in square pattern.

4- Results and discussions

4-1 Un-piled rafts results

This series studies the behavior of the un-piled raft under vertically uniformly distributed loads and moments. Table 4 shows the results of the analysis conducted in specified directions of the raft. There is a maximum total settlement of 173.3 mm and a 7 mm differential settlement for the raft. The large total settlement value is related to the soil layers' profile, consisting of silty clay and loose to medium-density silty sand. Generally, in foundation engineering design, according to ASCE 1997, the values of the allowable limits for total settlement are 75–125 mm in rafts on clay soil, and about 50–75 mm in rafts on sand Baban (2016), Holtz (1991); and for differential settlement are 20–60 mm and 1:500 as angular distortions Ryul et al. (2012), Holtz (1991). Thus, according to those limits, the settlement of a 2.0 m thick un-piled raft is not safe concerning the design requirement for raft foundation. Therefore, in the following phases of this study, pile installations will be used as the best option to limit the settlement value developed in the soil.

Fig. 8 shows the load settlement of the unpiled raft. According to this figure, the higher settlement ratio is observed at the edge of the raft, while its corner and center sides are ranked in the second and third places, respectively.

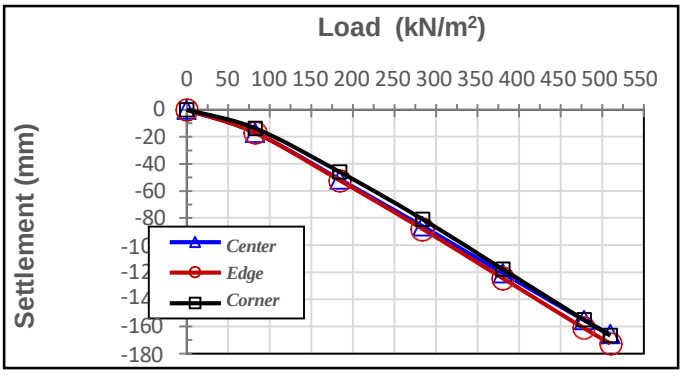

Fig. 8 Load-settlement relationships at different locations of the un-piled raft

Table 4: Unpiled raft results.

Case study	Value	Axial forces (kN/m)		Shear forces (kN/m)			Bending momen (kN-m/m)			Vertical displacement (mm)	Differential settlement (mm)
		N1	N2	Q12	Q23	Q13	M11	M22	M12		
Unpiled raft	Max.	647.7	731.3	141.6	2705	5307	8598	11310	4147	173.3	7
	Min.	142.8	118	-165.3	-8206	-2699	-3122	-7824	-5254		

4-2 Pile group foundation results

4-2-1 Effect of pile number and spacing

Table 5 summarizes the results of all studied cases (i.e., 24, 40, and 60 piles) of pile rafts as maximum values of total and differential settlement and raft bending moments. The table shows that as the pile number increased or pile spacing decreased, the total settlements decreased, and differential settlements increased. This behavior occurred due to the moment acting on the center of the raft foundation. It appears that the total displacement values in all pile rafts are quite different when s/d_{pile} decreases from 5 to 3 or the pile numbers increase from 24 to 60. A more uniform distribution of load with an increase in pile numbers or a decrease in pile spacing results in an improvement in settlement as the displacement pattern extends both in the x and y directions. In contrast, Tang et al. (2014) report that when s/d_{pile} > 5, each raft and pile behave independently, enabling all piles to reach their maximum carrying capacities. Fig. 9 shows how pile number and spacing affect pile raft responses in terms of load-settlement relationships.

Table 5: 3D analysis results of the pile raft foundations

Case study	Piles number and pattern	s / d_{pile}	l / d_{pile}	Total settlement (mm)	Differential settlement (mm)	Raft bending moment (MN.m/m)
Equal length	24 Square	5	12	99.5	2	7.5
			16	36.0	6	7.0
			20	32.3	6	7.1
Equal length	40 Square	4	12	62.4	7	15.1
			16	31.3	10	14.6
			20	28.0	10	14.6
Equal length	60 Square	3	12	45.1	4	10.8
			16	28.3	6	11.3
			20	25.7	7	10.0

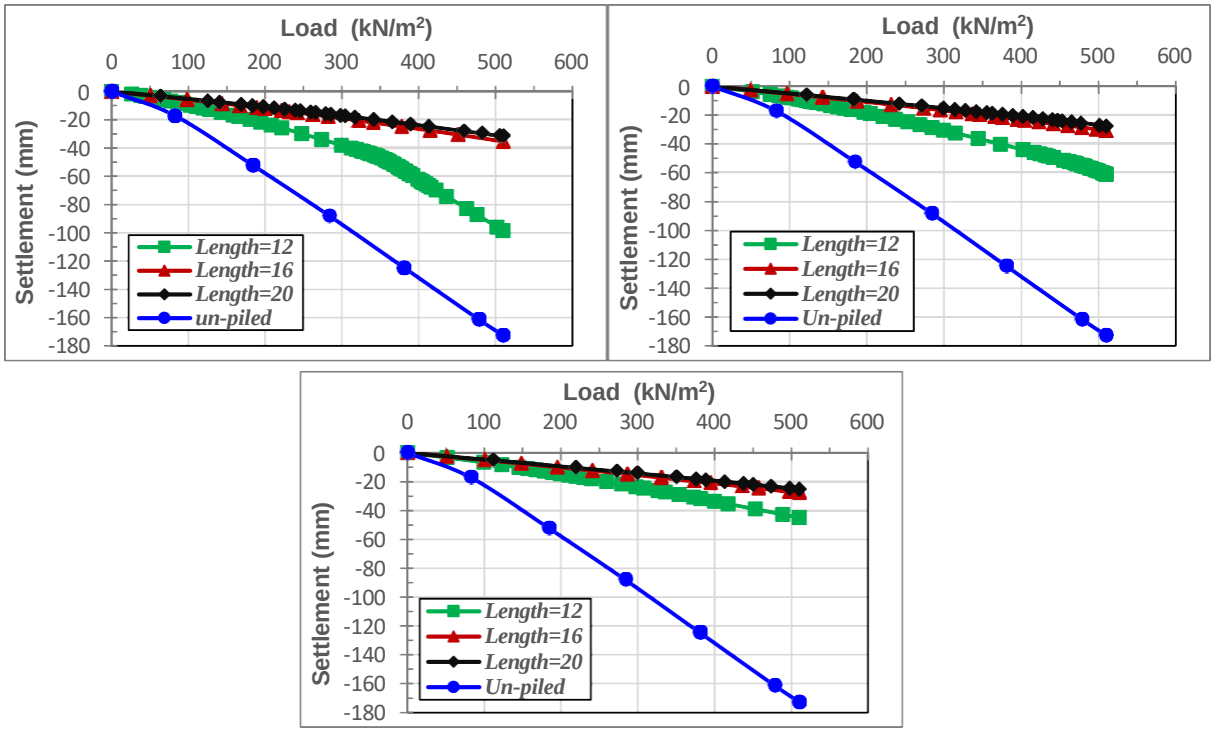

Fig. 9 Effect of pile spacing on the settlement.

4-2-2 Effect of pile length

The influence of pile length on pile raft response is described in terms of load-settlement relations shown in Fig. 10. Referring to Table 5 mentioned previously, it is seen that with increasing pile length, the vertical displacement decreases, and this in turn, at a specified spacing between the piles, affects the developed rafts' bending moment. The improved behavior in piled rafts is related to the overlap of soil pressures produced by the piles' shaft resistance or tip-bearing at closely spaced piles. Additionally, it is observed that 24 pile groups, 40 pile groups, and 60 pile groups have the greatest influence on load transfer from a raft to piles and subsoil. Conversely, soils that experience high soil pressures will fail to deform under shear or settle excessively (Al-Ne'aimi and Al-Brifkani 2016). Fig. 11 depicts sectional views of the development of soil partial collapses or plastic zones with depth under the influence of surface load and moment for unpiled and piled-raft foundations of varying pile lengths.

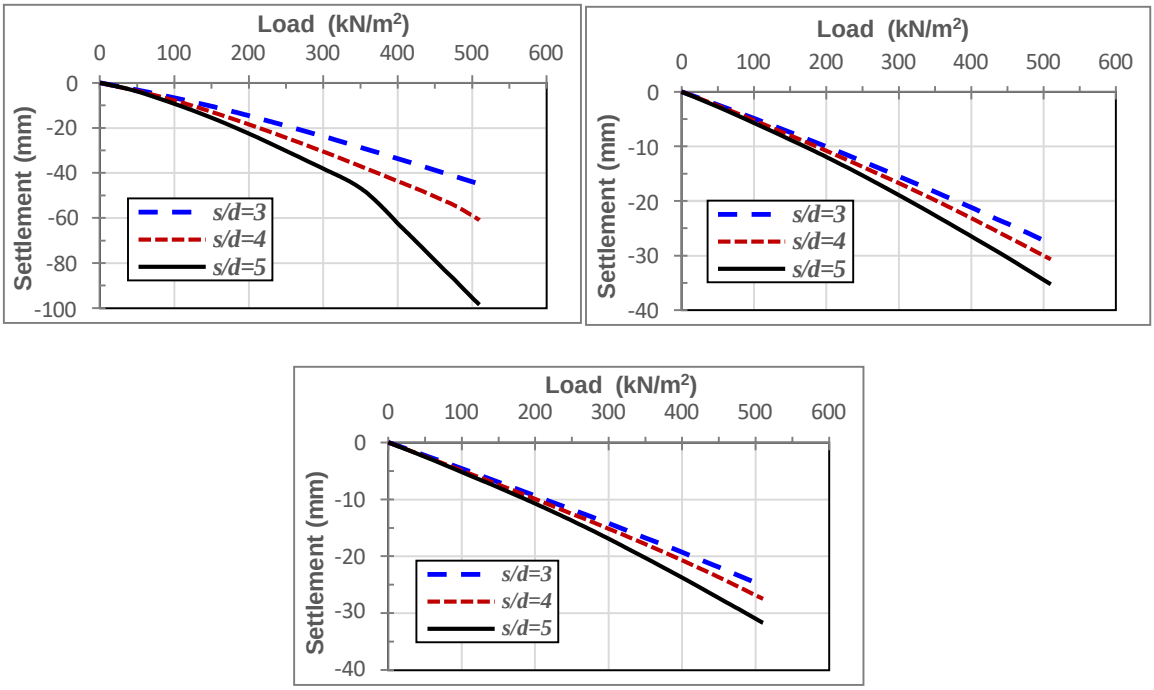

Fig. 10 Effect of pile length on the settlement.

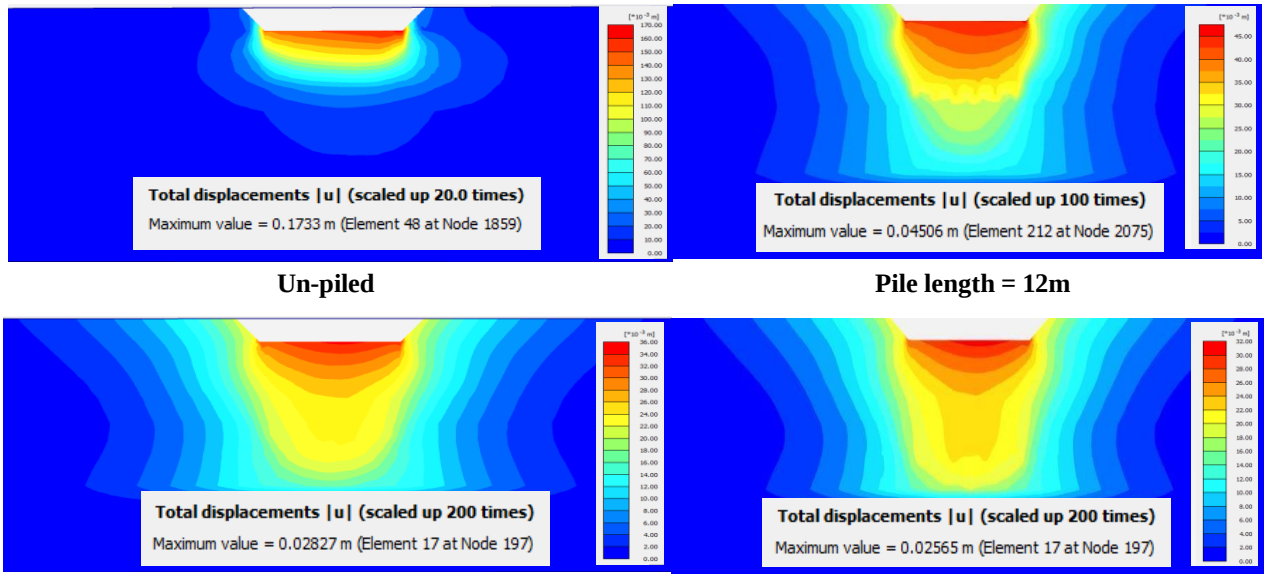

Un-piled **Pile length = 12m**

Pile length = 16m **Pile length = 20m**

Fig. 11 Sectional views of soil plastic zones for un-piled and piled raft foundations of equal length- square pattern with s/d = 3.

4-2-3 Load sharing between raft, pile, and subsoil

A raft's load is calculated after the summation of all the loads on top of each pile is subtracted from the total applied load. As shown in Table 6, each pile or raft is capable of carrying out a different load ratio. By increasing pile length from 12 to 20, the average load applied to the pile heads increases, illustrating the effect of pile spacing, pile number, and pile length on the load ratio absorbed by the raft, piles, and subsoil.

More precisely, concerning the raft load-sharing ratio, the total load carried by it decreases with higher numbers and lengths of piles. The average load (4801 kN) on each pile in the raft is higher than the allowable pile capacity because of excessive settlements in the raft. Further, a safety factor of 2.5 allows the raft's load-sharing ratio to be calculated when the pile load approaches its allowable capacity. As a result of applying the load to pile-raft groups with a 2.0 m raft thickness, Fig. 12 shows the distribution of raft load percentages for pile-raft groups.

4-2-4 Piles' shaft and tip resistance profiles

For all cases analyzed, Table 7 presents the ratios of shaft resistance and end-bearing along pile lengths and tips. In the study, it can be seen that the resistance ratios of the pile shaft and tip change when the pile number is increased from 24 to 40 or 60. Due to the large circumference and cross-sectional area of large piles, shaft resistance increases as the number and length of piles increase. However, for s/dpile < 5, the shaft resistance ratios developed along the pile lengths are higher than the tip resistance ratios. All studied cases have the same observation, which is related to pile group action. The end-bearing reaction $R_{base} = N_{bottom}$ is calculated based on the normal force values N obtained from the Plaxis output results. Similarly, the skin friction $R_{skin} = N_{top} - N_{bottom}$ is calculated based on the pile head load N_{top}. Based on a 2.0 m thick raft under the applied load, Fig. 13 shows the percentages of shaft and tip resistance loads.

Table 6: Load distribution of raft and piles with their skin friction and end-bearing.

Case study	Pile No.	s/d_{pile}	l/d_{pile}	Pile load %	Raft load %	R_{base} %	R_{skn} %
Equal length	24 Piles	5	12	41	59	74	26
			16	75	25	74	26
			20	77	23	63	37
Equal length	40 Piles	4	12	66	34	73	27
			16	83	17	62	38
			20	85	15	45	55
Equal length	60 Piles	3	12	78	22	66	34
			16	87	13	53	47
			20	87	13	33	67

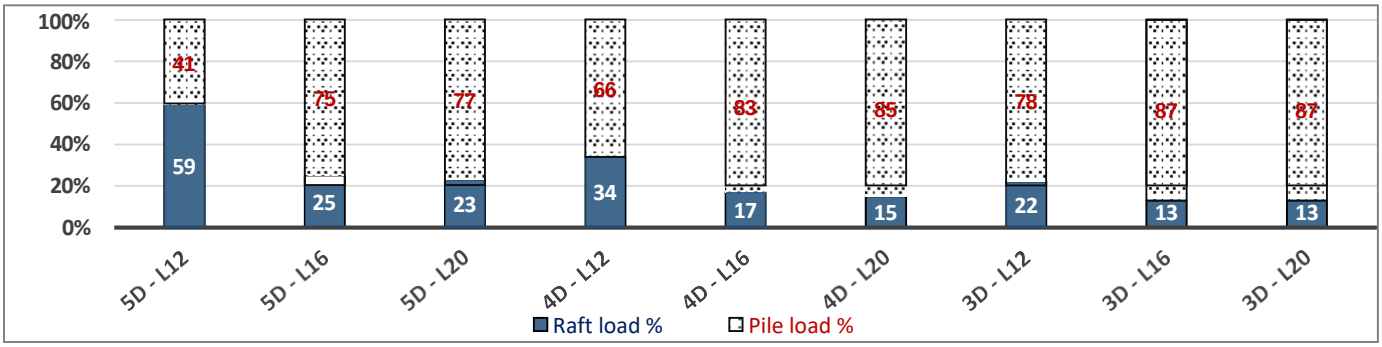

Fig. 12 Raft and pile load transfer ratios.

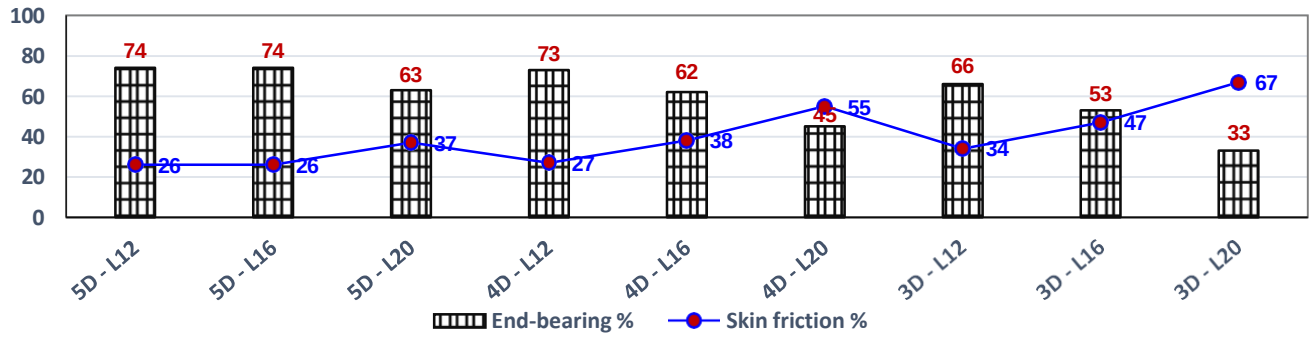

Fig. 13 Shaft and tip-bearing load ratios for several piles from all pile raft groups.

Table 7: Shaft and tip resistance loads for several piles from all pile raft groups (t_{raft}= 2m and d_{pile}=1m).

study	Pile number	s/d_{pile}	l/d_{pile}	R_{skin} * and R_{base} ** [KN]			$N_{Top} = R_{skin} + R_{base}$ [kN]			$\frac{R_{skin}}{R_{base}}$
				Corner pile	Edge pile	Center pile	Corner pile	Edge pile	Center pile	
Equal length	24 piles	5	12	1447* 4119**	1433 4118	1430 4116	5566	5551	5546	0.351 0.348 0.347
			16	2631 9231	2632 8069	2662 7490	11862	10701	10152	0.285 0.326 0.355
			20	3949 7690	3900 7022	3892 6135	11639	10922	10027	0.513 0.555 0.634
Equal length	40 piles	4	12	1422 3808	1421 4117	1445 4118	5230	5538	5563	0.373 0.345 0.350
			16	2621 4291	2567 5557	2570 4158	6912	8124	6728	0.610 0.462 0.618
			20	3710 3155	3834 4294	3842 3187	6865	8128	7029	1.176 0.892 1.205
Equal length	60 piles	3	12	1470 3018	1453 2616	1443 2711	4488	4069	4154	0.487 0.555 0.532
			16	2597 3508	2613 3051	2354 1988	6105	5664	4342	0.740 0.856 1.184
			20	3540 2733	3817 2436	3086 1210	6273	6253	4296	1.295 1.567 2.550

As illustrated in Fig. 14, 24 pile group foundations were tested for skin friction and end-bearing loads. Almost equal load ratios were observed for piles positioned at the corners, edges, and center with a pile length of 12 m and a spacing of s/d_{pile} = 5. But, for the same 4x6 pile group, with increasing pile lengths to 16 m or 20 m, the higher axial load is absorbed by the corner piles, followed by those of the edge and center piles. Such behavior is related to increasing l/d_{pile} ratios, which increase the values of shaft and tip resistance compared to those with pile lengths of 12 m. The pile shaft and tip resistance loads at different pile locations from all pile raft groups in square patterns are presented in Table 7.

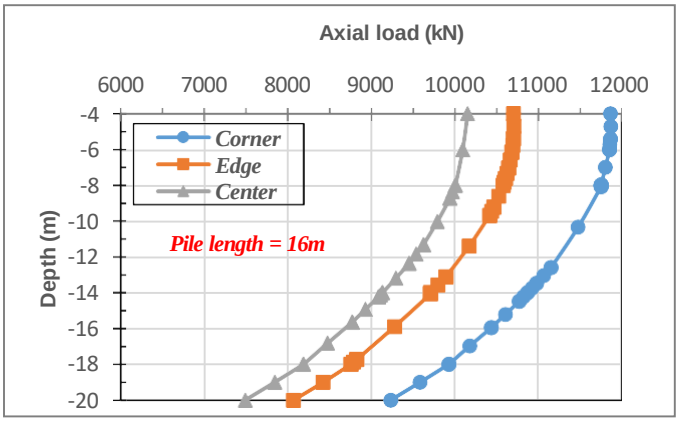

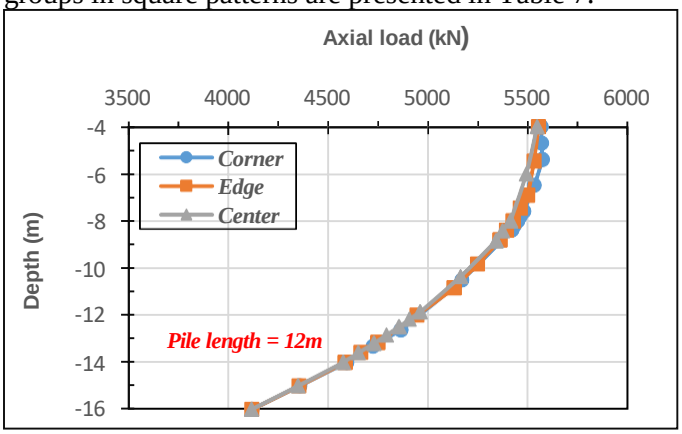

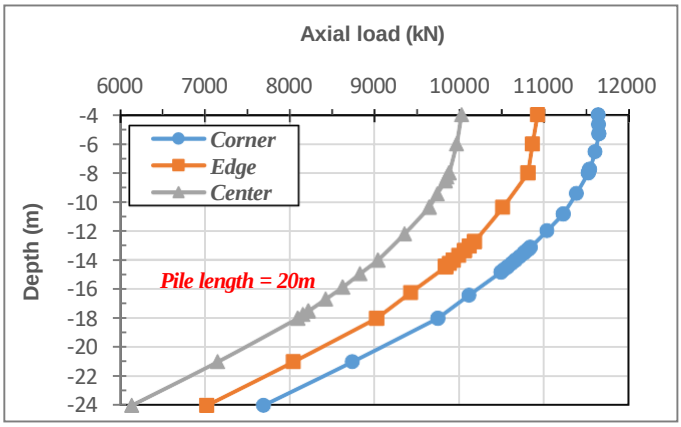

Fig. 14 Axial load distribution along pile lengths for 24 pile group (s/d_{pile}= 5).

In general, pile spacing, pile length, pile numbers, and raft thickness significantly affect the load sharing between rafts and piles. Table 7 shows that piles of 20 m in length enhance their load-carrying capacity more than piles of 12 m in length do by mobilizing their skin resistance. On the other hand, piles can mobilize their capacities fully when placed with a higher spacing s/d_{pile} = 5 under the raft, irrespective of the length of the piles. In this case, the stress fields of the pile's overlap become minimal.

4-2-5 Effect of moment load

In all cases of the study, the raft is subjected to a vertical load in the direction of gravity as a distributed load of 510 kN/m2 and large moments Mx = −50000 kN-m, and My = 30000 kN-m applied on the first quarter of the foundation. In this scenario, the 24, 40, and 60-pile group foundations of 16 m length were studied under vertical load and moments as well as a purely vertical load for comparison. The results of the analyses of each pile group under both loading cases are shown in Table 8.

As shown in Table 8 for all pile groups considered, the comparison of the results of both cases of loading shows that the moment load has approximately no effect on the raft's settlement or the shaft and tip resistance of the piles, whereas the raft's bending moment and the load sharing ratios between the raft and the piles are significantly affected. It appears that when the raft foundation is subjected to a combined vertical load and moments, the raft's bending moment increased by about 2.2, 5.4, and 6.1 ratios, and the raft load absorption increased by 1.4, 1.7, and 2.2 ratios, respectively compared to that without moments for 24, 40, and 60 pile groups, respectively, whereas the pile load decreased by 91% for all studied pile groups. On the other hand, with increasing pile numbers from 24 to 60 or decreasing pile spacing (s) from $5d_{pile}$ to $3d_{pile}$, the load absorbed by the raft decreased from 25% to 13%, in contrast to an increase in the load pile ratios from 75% to 87%.

Fig. 15 shows the 3D pile load distribution for 6x10 piles under different loading conditions. The large disparity in load distribution in this pile group foundation is due to a sudden increase in forces at the corner piles, where the maximum force is found as a result of overturning moments. Furthermore, under purely vertical load, the load distribution in piles is symmetrical about both the x-and y-axes. The same observation is noticed with the combined vertical load and the large moment regarding the sudden increase in exterior piles, especially in corner piles, due to mobilized shaft resistance. This result supports the findings of the previous works by Comodromos et al. (2009, Engin et al. (2008).

Table 8: Effect of moment load on the pile groups response.

Parameter	24 piles		40 piles		60 piles	
	Surface load plus moment	Surface load	Surface load plus moment	Surface load	Surface load plus moment	Surface load
Settlement (mm)	36.0	35.1	31.3	30.6	28.3	27.7
Differential settlement (mm)	6	7	10	11	7	7
Raft max. bending moment (kN.m/m)	7000	3238	14685	2726	11329	1863
Pile load %	75	82	83	90	87	94
Raft load %	25	18	17	10	13	6
R_{base} %	74	74	62	62	53	53
R_{skin} %	26	26	38	38	47	47

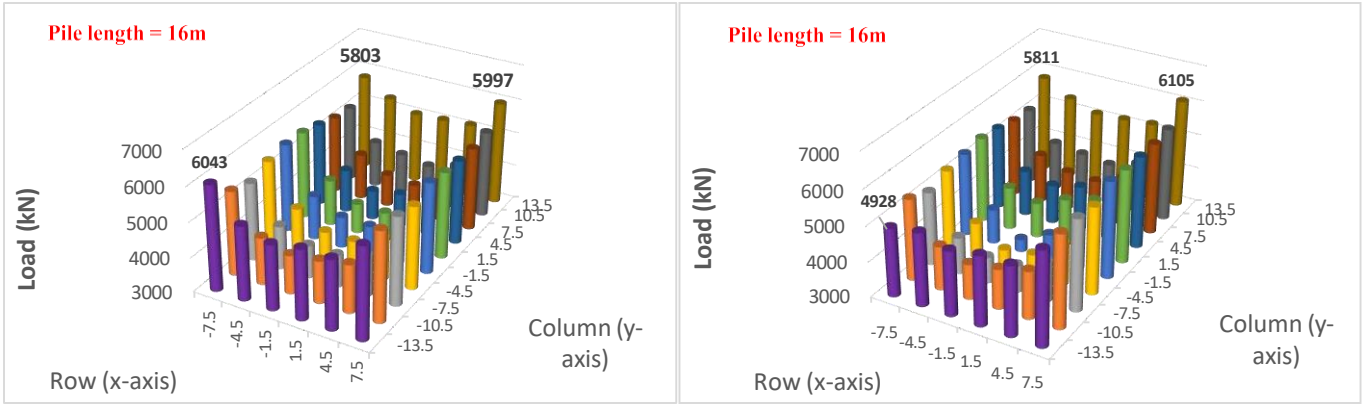

Surface load **Moment and surface loads**

Fig. 15 3D pile load distribution for 6x10 piles under different loading conditions.

5- Conclusions

This study highlights the performance of a pile raft foundation embedded in layered clay soil under a combined vertical load and large moments using PLAXIS 3D. The key concluding points from the analysis of the presented work are:

- As the pile number increased in pile rafts, total settlements at the rafting center decreased while differential settlements increased.
- For a specified spacing between the piles, the raft bending moment decreases with increasing pile length. All cases studied exhibit this behavior.
- Load settlement, bending moments within the pile cap or raft, and load sharing between the raft, piles, and subsoil are strongly influenced by the length and spacing between piles. In addition to increasing the average load carried by piles, higher numbers and lengths of piles result in a decrease in the load carried by the raft.
- Piles, regardless of length, can mobilize full capacities when placed at a higher spacing (s) > $5d_{pile}$ under the raft.
- There is a strong correlation between the shaft and tip resistance of piles along their lengths and tips and the pile number, spacing, length, and location, whether they are corner, edge, or center piles. Both skin friction and end-bearing ratios increase with an increase in pile length or pile spacing. As a result of load redistribution on the piles, skin friction increases more rapidly than end-bearing.
- The moment load effects increased the bending moment in the raft by 2.2%, 5.4%, and 6.1%, and the raft load absorption by 1.4%, 1.7%, and 2.2% compared to those without moments for 24, 40, and 60 pile groups, respectively, whereas the pile load decreased by 91% for all studied groups.

In the case of pure vertical load, the pile load distribution is symmetrical about both the x and y axes, compared to an unsymmetrical one in the case of combined vertical load and moments resulting from the sudden increase, especially in corner piles, due to mobilized shaft resistance.

6- Recommendations for future research

- Developing a mathematical expression using an Artificial Neural Network (ANN) that describes the load distribution of each pile within the pile raft group under vertical load and large moments.
- It is recommended to compare the 3D numerical analysis results of pile raft foundations with the monitoring data of a case study or full-scale models.
- Performing extensive research on pile group foundations under different load eccentricities.

7- Conflicts of Interest

The authors declare that they have no financial and personal relationships of any nature with any product, service, and/or company regarding the publication of this paper."

8- References

Abdel-Fattah, T. and A. Hemada (2014). Use of creep piles to control settlement of raft foundation on soft clay—case study. Proceedings of 8th Alexandria international conference on Structural and geotechnical engineering, Alexandria.

Al-Ne'aimi, S. and M. S. Hussain (2021). "Numerical modeling and parametric study of piled rafts foundations." Arabian Journal of Geosciences **14**(6): 1-13.

Baban, T. M. (2016). Shallow foundations: discussions and problem-solving, John Wiley & Sons.

Bathe, K. (1996). An Introduction to the Use of the Finite Element Procedures in Finite Element Procedures, Prentice-Hall, Englewood Cliffs, New Jersey, USA.

Choudhury, D., R. Shen and C. Leung (2008). Centrifuge model study of a pile group subject to Adjacent excavation. GeoCongress 2008: Characterization, Monitoring, and Modeling of GeoSystems**:** 141-148.

Comodromos, E. M., C. T. Anagnostopoulos and M. K. Georgiadis (2003). "Numerical assessment of axial pile group response based on the load test." Computers and Geotechnics **30**(6): 505-515.

Comodromos, E. M., M. C. Papadopoulou and I. K. Rentzeperis (2009). "Pile foundation analysis and design using experimental data and 3-D numerical analysis." Computers and Geotechnics **36**(5): 819-836.

Davids, A., J. Wongso, D. Popovic and A. McFarlane (2008). A Postcard from Dubai's design and construction of some of the tallest buildings in the world. Proc. of the CTBUH 8th World Congress.

Elwakil, A. and W. Azzam (2016). "Experimental and numerical study of piled raft system." Alexandria Engineering Journal **55**(1): 547-560.

Engin, H., E. Septanika and R. Brinkgreve (2007). "Improved embedded beam elements for the modeling of piles."

Engin, H., E. Septanika and R. Brinkgreve (2008). Estimation of pile group behavior using embedded piles. Proceeding of the 12th International Conference of International Association for Computer Methods and Advances in Geomechanics, Goa, India.

Engin, H., E. Septanika, R. Brinkgreve and P. Bonnier (2008). Modeling piled foundations using embedded piles. Geotechnics of Soft Soils: Focus on Ground Improvement, CRC Press**:** 143-148.

Fioravante, V. and D. Giretti (2010). "Contact versus noncontact piled raft foundations." Canadian Geotechnical Journal **47**(11): 1271-1287.

Gebregziabher, H. F. and R. Katzenbach (2012). Parametric studies on the application of CPRF on semi-soft stratified soils. GeoCongress 2012: State of the Art and Practice in Geotechnical Engineering**:** 125-134.

Holtz, R. D. (1991). Stress distribution and settlement of shallow foundations. Foundation engineering handbook, Springer**:** 166-222.

Li, B., C. Jia, G. Wang, J. Ren, G. Lu and N. Liu (2020). "Numerical Analysis on the Performance of the Underwater Excavation." Advances in Civil Engineering **2020**.

Likitlersuang, S., C. Surarak, D. Wanatowski, E. Oh and A. Balasubramaniam (2013). "Finite element analysis of a deep excavation: A case study from the Bangkok MRT." Soils and Foundations **53**(5): 756-773.

Obrzud, R. F. (2010). "On the use of the Hardening Soil Small Strain model in geotechnical practice." Numerics in geotechnics and structures **16**: 1-17.

Prakoso, W. A. and F. H. Kulhawy (2001). "Contribution to piled raft foundation design." Journal of Geotechnical and geoenvironmental engineering **127**(1): 17-24.

Rabiei, M. (2010). Effect of pile configuration and load type on piled raft foundations performance. Deep Foundations and Geotechnical In Situ Testing**:** 34-41.

Ryltenius, A. (2011). "FEM Modelling of piled raft foundations in two and three dimensions." TVGT.

Ryul, K. S., C. S. Gyo, N. T. Dung and B. H. Fellenius (2012). "Design for Settlement of Pile groups by the unified design method. A case history." Full-Scale Testing and Foundation Design. doi https://doi.org/10.1061/9780784412084.0039.

Sales, M. M., M. Prezzi, R. Salgado, Y. S. Choi and J. Lee (2017). "Load-settlement behavior of model pile groups in the sand under vertical load." Journal of Civil Engineering and Management **23**(8): 1148-1163.

Sivrikaya, O. and Y. Gurkan (2019). "Two-and three-dimensional analyses of the effect of pile spacing in piled-raft foundations." Acta Geogr Slov **16**(1): 43-52.

Tang, Y., J. Pei and X. Zhao (2014). "Design and measurement of piled-raft foundations." Proceedings of the Institution of Civil Engineers-Geotechnical Engineering **167**(5): 461-475.

Tomlinson, M. and J. Woodward (2007). Pile design and construction practice, CRC press.

Viggiani, C., A. Mandolini and G. Russo (2012). "Piles and pile groups." Applied Soil Mechanics: 286-331.